

# SANDIA REPORT

SAND2019-9323

Printed August 2019



Sandia  
National  
Laboratories

# Demonstration of Metallic Coatings for High Durability Polymer BAAM Tooling

Andrew W Vackel  
Andrew S Miller

Prepared by  
Sandia National Laboratories  
Albuquerque, New Mexico  
87185 and Livermore,  
California 94550

Issued by Sandia National Laboratories, operated for the United States Department of Energy by National Technology & Engineering Solutions of Sandia, LLC.

**NOTICE:** This report was prepared as an account of work sponsored by an agency of the United States Government. Neither the United States Government, nor any agency thereof, nor any of their employees, nor any of their contractors, subcontractors, or their employees, make any warranty, express or implied, or assume any legal liability or responsibility for the accuracy, completeness, or usefulness of any information, apparatus, product, or process disclosed, or represent that its use would not infringe privately owned rights. Reference herein to any specific commercial product, process, or service by trade name, trademark, manufacturer, or otherwise, does not necessarily constitute or imply its endorsement, recommendation, or favoring by the United States Government, any agency thereof, or any of their contractors or subcontractors. The views and opinions expressed herein do not necessarily state or reflect those of the United States Government, any agency thereof, or any of their contractors.

Printed in the United States of America. This report has been reproduced directly from the best available copy.

Available to DOE and DOE contractors from

U.S. Department of Energy  
Office of Scientific and Technical Information  
P.O. Box 62  
Oak Ridge, TN 37831

Telephone: (865) 576-8401  
Facsimile: (865) 576-5728  
E-Mail: [reports@osti.gov](mailto:reports@osti.gov)  
Online ordering: <http://www.osti.gov/scitech>

Available to the public from

U.S. Department of Commerce  
National Technical Information Service  
5301 Shawnee Rd  
Alexandria, VA 22312

Telephone: (800) 553-6847  
Facsimile: (703) 605-6900  
E-Mail: [orders@ntis.gov](mailto:orders@ntis.gov)  
Online order: <https://classic.ntis.gov/help/order-methods/>



## ABSTRACT

The ability to print polymeric materials at a high volume rate ( $\sim 1000 \text{in}^3/\text{hr}$ ) has been demonstrated by Oak Ridge National Lab's (ORNL) Manufacturing Demonstration Facility (MDF) and shows promise for new opportunities in Additive Manufacturing (AM), particularly in the rapid fabrication of tooling equipment for prototyping. However, in order to be effective, the polymeric materials require a metallic coating akin to tool steels to survive the mechanical and thermal environments for their intended application. Thus, the goal of this project was to demonstrate a pathway for metallizing Big Area Additive Manufactured (BAAM) polymers using a Twin Wire Arc (TWA) spray coating process. Key problems addressed in this study were the adhesion of sprayed layers to the BAAM polymer substrates and demonstration of hardness and compression testing of the metallized layers

## **ACKNOWLEDGEMENTS**

The authors would like to acknowledge:

Mark Smith, Deidre Hirschfeld, and Pylin Sarobol for bringing the project to the attention of the Thermal Spray Research Lab at Sandia National Labs and assistance with proposal writing

Christina Profazi for metallographic preparation of samples and hardness testing

Bonnie Mckenzie for microscopy work

Members of the Thermal Spray Research Lab at Sandia for their universal support and assistance with maintaining and operation of the lab's facilities

Sandia National Laboratories is a multi-mission laboratory managed and operated by National Technology & Engineering Solutions of Sandia, LLC, a wholly owned subsidiary of Honeywell International Inc., for the U.S. Department of Energy's National Nuclear Security Administration under contract DE-NA0003525.

This Oak Ridge National Laboratory (ORNL) Manufacturing Demonstration Facility (MDF) project was funded by the US Department of Energy (DOE), Office of Energy Efficiency and Renewable Energy (EERE) Advanced Manufacturing Office (AMO). This project was managed as proposal number IEW018190325. The lead organization was the Oak Ridge National Laboratory (ORNL).

## CONTENTS

1. INTRODUCTION .....	9
1.1. Project Objective.....	9
1.2. Project Background .....	9
2. RESULTS AND DISCUSSION.....	11
2.1. Task 1: Baseline Electric Arc Spray Process.....	11
2.1.1. Materials and Methods .....	11
2.1.2. Initial Spray Trials .....	13
2.1.3. Coating Microstructure and Hardness Characterization.....	15
2.2. Task 2: Optimize Electric Arc Spray Process for Low Coating Residual Stress and High Adhesion Strength .....	17
2.2.1. Residual Stress Characterization .....	18
2.2.2. Optimization for Coating Adhesion .....	20
2.2.3. Coating Roughness .....	21
2.3. Task 3: Fabrication and Compression Testing of Simple Geometry Tooling .....	22
2.3.1. Compression Test by Brinell Indentation .....	22
2.3.2. Fabrication of Coating on Simple Geometry Tooling .....	24
3. Accomplishments and Conclusions .....	26
3.1. Patents .....	26
3.2. Publications and Presentations .....	26
3.3. Recommendations .....	26
4. References .....	27
Appendix A. Main Appendix Title.....	29
A.1. Sub-Appendix Title .....	29

## LIST OF FIGURES

Figure 1: 3D printed ABS mold cavity before and after coating with Kirkosite alloy, and the cross-sectional coating microstructure from SAND2015-8462. ....	11
Figure 2: Schematic of the Twin Wire Arc (TWA) coating process (Image from Oerlikon-Metco). ....	12
Figure 3: Praxair 8835 Twin Wire Arc Gun. ....	13
Figure 4: Image of ABS/CF-20% and PPS/CF-50% BAAM substrates to be used for spray trials. ....	14
Figure 5: Top surface images of ~25.4mm x ~229mm ABS/CF-20% BAAM substrates coated with Vecalloy B, Zinc, and Aluminum with varying degrees of adhesion and coating integrity. ....	15
Figure 6: Cross section micrograph of the interface between TWA Zinc coating and the ABS/CF-20% BAAM substrate. The Zinc coating readily infiltrates the roughness of the BAAM material that is native to the printing process, promoting mechanical adhesion. ....	15
Figure 7: Cross section SEM micrograph of thick TWA Zinc coating. ....	16
Figure 8: Cross section SEM micrographs of the "WC Amorphous" and "Amorphous Alloy" coatings. ....	17
Figure 9: Average Vickers hardness measured for the "Amorphous Alloy" and "WC Amorphous" coating top surfaces with error bars showing the standard deviation. ....	18
Figure 10: Average Vickers hardness measured for the "Amorphous Alloy" and "WC Amorphous" coating cross sections with error bars showing the standard deviation. ....	18
Figure 11: ICP measurements for TWA sprayed Zinc onto Aluminum (a) Curvature vs. time and (b) backside substrate temperature vs. time. Measurements were taken simultaneously during coating deposition and cooling. ....	20

<i>Figure 12: ICP measurements for TWA sprayed “WC Amorphous” wire onto TWA Zinc coated Aluminum (a) Curvature vs. time and (b) backside substrate temperature vs. time. Measurements were taken simultaneously during coating deposition and cooling .....</i>	20
<i>Figure 13: ICP measurements for TWA sprayed “WC Amorphous” wire onto TWA Zinc coated Aluminum (a) Curvature vs. time and (b) backside substrate temperature vs. time. Measurements were taken simultaneously during coating deposition and cooling .....</i>	21
<i>Figure 14: Top surfaces of BAAM Polymer coupons that we sprayed with Vecalloy B with no Zinc bond coat, a thin Zinc bond coat, and a thick Zinc bond coat.....</i>	22
<i>Figure 15: Sample where the Zinc bond coat was machined on half of the surface prior to top coat application. ....</i>	22
<i>Figure 16: Sample of metallized BAAM Polymer with a Zinc bond coat that has been machined flat, followed by a polishing “Amorphous Alloy” top coat.....</i>	23
<i>Figure 17: Sample plate that highlights the steps of a proposed stack up for BAAM metallization.....</i>	23
<i>Figure 18: Representative Strain vs. Mean Pressure for coated and un-coated PPS/50% CF BAAM Polymer.....</i>	25
<i>Figure 19: Convex (Left) and Concave (Right) simple geometry tooling blocks BAAM printed in PPS/CF-50%.....</i>	25
<i>Figure 20: Simple geometry tooling block after Zinc coating. ....</i>	26

## LIST OF TABLES

<i>Table 1: List of wire feedstock material used for feasibility study.....</i>	13
---	----

This page left blank

## EXECUTIVE SUMMARY

### Objective and Tasks.

The primary objective of this project was to demonstrate the feasibility of using Twin Wire Arc (TWA) as a thermal spray method to apply hard metallic-based coatings to Big Area Additively Manufactured (BAAM) polymeric materials for rapid tool forming applications. Tasks included baselining the TWA process and demonstrating adhesion to polymeric substrates, optimizing the coating process for strong coating adhesion, and demonstrating the ability to coat relevant tooling geometries.

### Results and Conclusions.

A multi-layered coating approach was demonstrated using a Zinc bond coat that allows for hard-facing top coat materials to then be applied. Attempts of adhering the hard-facing materials directly onto the polymers were un-successful. In addition to the lower processing temperature of Zinc coating, it is thought that the low residual stress and relaxation of the Zinc bond coat allows the higher residual stress top coat materials to adhere. The rough as-printed beaded surfaces of the BAAM polymer were thought to aid adhesion of the Zinc bond coat through additional mechanical interlocking. Machining of the Zinc followed by hard-facing coating application was demonstrated to create flat coating surfaces, though as-deposited coatings contained appreciable roughness.

Vickers indentation testing at 300g of hard-facing materials resulted in Vickers harnesses of  $642 \pm 190$  for an Iron-based alloy and  $590 \pm 195$  for a second Iron-based alloy with Tungsten Carbide particle inclusions, which equate to  $\sim 55$  Rockwell C hardness. An over-test scenario using Brinell indentation compression testing of the multi-layered coating on BAAM Polymers showed good adhesion in coatings having a higher hardness than Polyphenylene Sulfide with 50% Carbon Fiber loading (PPS/CF-50%). Cracking was observed in the Acrylonitrile Butadiene Styrene with 20% Carbon Fiber loading (ABS/CF-20%) substrates during the test in both the coated and un-coated samples.

*In conclusion, a pathway for successful hard-facing metallization of BAAM polymers has been demonstrated using the TWA process that allows surface hardening with strong adhesion*

## ACRONYMS AND DEFINITIONS

Abbreviation	Definition
ABS	Acrylonitrile Butadiene Styrene
AM	Additive Manufacturing
AMO	Advanced Manufacturing Office
BAAM	Big Area Additive Manufacturing
CF	Carbon Fiber
CTE	Coefficient of Thermal Expansion
DOE	Department of Energy
EDS	Electron Dispersive Spectroscopy
EERE	Office of Energy Efficiency and Renewable Energy
HRC	Rockwell Hardness C
HV	Vickers Hardness
ICP	In-situ Coating Property
MDF	Manufacturing Demonstration Facilities
ORNL	Oak Ridge National Lab
PPS	Polyphenylene Sulfide
RA	Roughness Average
SEM	Scanning Electron Microscope
SNL	Sandia National Labs
TSRL	Thermal Spray Research Lab
TWA	Twin Wire Arc

## 1. INTRODUCTION

### 1.1. Project Objective

The combination of the Big Area Additive Manufacturing (BAAM) and thermal spray coating technologies were used to demonstrate direct manufacture of higher strength and wear-resistant tooling, with acceptable surface finish, at very high rates. The main objective for this proposal is to investigate and demonstrate developed thermal spray technologies for low residual stress metallic coatings as a coating solution for the Manufacturing Demonstration Facilities/Oak Ridge National Laboratory (MDF/ORNL) 3-D printed polymer composite BAAM parts and tools. The primary attribute of concern in this preliminary project is the adhesion of the coating to the substrate fiber reinforced polymer and hardness values of 65 to 68 Rockwell C for the coating surfaces.

The objectives of this work were broken down as indicated below

#### Task 1: *Baseline Electric Arc Spray Process*

This task was to demonstrate a tool steel/ high strength alloy coating that adheres to flat CF-polymer BAAM substrates.

#### Task 2: *Optimize Electric Arc Spray Process for Low Coating Residual Stress and High Adhesion Strength*

This task was to demonstrate an optimized coating with low residual stress, high stiffness, and high adhesion strength and probing when edge delamination of the coating would occur

#### Task 3: *Fabrication and Compression Testing of Simple Geometry Tooling*

Fabrication of a simple test article as a demonstrator

### 1.2. Project Background

Manufacture of tooling for stretch form, hydroforming dies, and compression molding tools currently involves machining tool steel from billets with >3 months lead time and >\$100K. Rapid fabrication of tooling, using 3-D printed Big Area Additive Manufacturing (BAAM) polymer composite technology, has been shown successful by researchers at the Manufacturing Demonstration Facilities (MDF) at Oak Ridge National Laboratory (ORNL). Big Area Additive Manufacturing is creating a disruption in Additive Manufacturing (AM) by helping redefine the economics and applications of AM. Conventional AM systems are characterized by small scale (i.e. less than 1 cubic foot), slow deposition rates (i.e. typically 1 cubic inch/hour) and expensive feedstocks (i.e. greater than \$100/lb). BAAM enables rapid (i.e. greater than 1000 cubic inch/hour) production of large scale (i.e. greater than 100 cubic feet) using low cost feedstocks (i.e. less than \$5/lb). The combination of these characteristics can transform AM from a process with a net cost of \$1500/lb to \$3000/lb to under \$30/lb. While BAAM is rapidly maturing and finding multiple applications such as prototypes, composite tooling and dies, etc., the current machine limitations of planar deposition with three axis gantries introduce defects into material that result in low z-strength. MDF researchers are currently working on five axis deposition that should improve properties of printed structures and are interested in increasing wear resistance of the additively manufactured ABS/CF-20% by weight sheet metal forming tools and PPS/CF-50% by weight thermoplastic compression molding tools.

Metallic surface coatings can be applied to 3-D printed polymer composite BAAM tooling to

increase strength and wear-resistance. Researchers at the Thermal Spray Research Laboratory (TSRL) at Sandia National Laboratories (SNL) have previously demonstrated (*Figure 1*) that an electric arc spray, using Kirksite alloy (i.e., a family of low melting point Zinc / Aluminum alloys that have been reported as useful for making short run polymer injection molds), can be used to apply coatings to 3-D printed plastic parts. Today, SNL continues to develop thermal sprayed coating technologies for various applications. Electric arc spray allows integration of many coating materials including metallic alloys, metallic-ceramic composite, etc. with the 3-D printed polymer parts, as well as a high application rate ( $>160$  cubic in/hr). Wire feedstock for various metals of interest such as steel and chromium can be readily obtained and investigated as the surface coating for the polymer BAAM tooling to increase the tooling strength and increase the tooling usage. In addition, remanufacturing is possible by stripping the worn coatings from the substrates and reapplying fresh coatings.

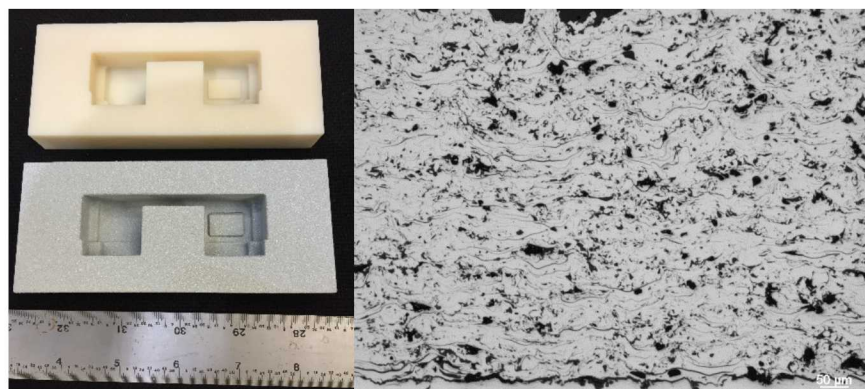


**Figure 1: 3D printed ABS mold cavity before and after coating with Kirksite alloy, and the cross-sectional coating microstructure from SAND2015-8462.**

## 2. RESULTS AND DISCUSSION

### 2.1. Task 1: Baseline Electric Arc Spray Process

#### 2.1.1. Materials and Methods

The TWA spray process was selected as the process of BAAM metallization based on two criteria. Primarily, the TWA process allows a much larger application rate of material at a lower cost as compared to other thermal spray processes that would be a better match for the BAAM printing process's volumetric printing rate. Additionally, the variety of materials that can be applied by the TWA process ranges from soft, low melting temperature materials (e.g., Zinc) to high melting temperature refractories (e.g., Molybdenum) and composite materials that contain hard ceramic inclusions (e.g., carbide-particle cored wire). The only feedstock selection constraint for the process is that the feedstock must be conductive. A schematic of the process is shown in *Figure 2*. The process consists of a dual feed of electrically biased wire feed stock that arcs and melts upon contact. An atomizing gas propels the molten droplets towards the substrate surface where the droplets impinge and quench onto the surface. The TWA process also has the advantage of not using a plasma or oxy-fuel plume as the heat source for melting the feedstock material like plasma or flame spray, respectively, thus eliminating convective heating of the substrate surface.

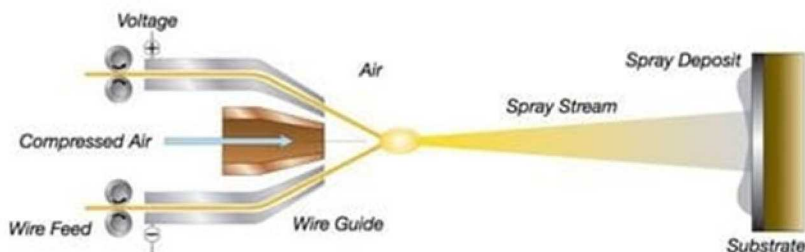


**Figure 2: Schematic of the Twin Wire Arc (TWA) coating process**  
(Image from Oerlikon-Metco).

There are several drawbacks of the TWA process for this application however. The first, the porosity associated with process, is readily observable in *Figure 1*. Nearly all thermal spray processes produce coatings with some degree of porosity but the low velocity of molten droplets in the TWA process compared to other higher velocity spray processes imposes a density limit. The second drawback of the TWA process is the residual coating stresses, which are typically tensile and may reduce coating adhesion when stress levels are too high or too thick a coating has been applied. Higher velocity processes may help neutralize these tensile stresses by a peening mechanism from high velocity particle impacts<sup>1</sup>. Lastly, the process results in a coating with a native roughness much higher than that of a machine quality finish and would require post process grinding and/or polishing. These drawbacks can be somewhat alleviated by higher velocity processes but were not considered for this feasibility study due to offsetting the long-term benefits of application rate and cost affordability for possible commercial use<sup>1</sup>.

---

<sup>1</sup> In the timeframe of the project, the authors became aware of a new commercial hybrid technology that combined wire spraying with a high velocity adaptation which may offer hybrid benefits of the processes.



**Figure 3: Praxair 8835 Twin Wire Arc Gun.**

A commercially available Praxair 8835 TWA spray system and the TSRL at SNL was used for all sample preparation (*Figure 3*). Nitrogen was chosen as the atomizing gas as opposed to air to reduce oxidation of molten droplets. Several commercially available wire feedstocks were experimented with and are detailed in *Table 1*.

**Table 1: List of wire feedstock material used for feasibility study**

Material	Composition	Vendor
Zinc	Zn (99.99%)	Tafa
Aluminum	Al (99.5%)	Tafa
Copper	Cu (98.0%)	Tafa
High Carbon Steel	Si (0.3wt%) C (0.8wt%) Mn (0.7wt%) Fe (Balance)	Polymet
“Vecalloy B”	Ni (5-10wt%) Cr (5-10wt%) Nb (5-10wt%) Al (0.1-5wt%) Si (0.1-5wt%) Mn (0.1-5wt%) B (0.1-5wt%) Fe (Balance)	Polymet
“Amorphous Alloy”	Cr (23.0wt%) Ni (9.0wt%) Mo (4.0wt%) B (2.3wt%) Cu (2.0wt%) Mn (1.3wt%) Si (1.0wt%) Fe (Balance)	Polymet
“WC Amorphous”	WC (26.0wt%) Cr (13wt%) TiC (6.0wt%) Ni (6.0wt%) B (2.0wt%) Si (1.0wt%) Fe (Balance)	Polymet

BAAM test substrates of ABS/CF-20% and PPS/CF-50% were provided by MDF that were approximately 25.4mm x 229mm (pictured in *Figure 4* ) to be compatible with ReliaCoat's In-situ Coating Property (ICP) sensor. The ICP sensor is a commercial device which monitors substrate curvature and backside temperature via non-contact displacement sensors and contact thermocouples, respectively, during the coating process that can be used to analyze residual stress evolution during coating and cooling. Details of the working theory behind the device is outlined in Reference [2]. Aluminum substrates of the same dimensions were used as well for coating development. Substrate surface to be coated were either left in their native finish or grit blasted with alumina media.



**Figure 4: Image of ABS/CF-20% and PPS/CF-50% BAAM substrates to be used for spray trials.**

### **2.1.2. Initial Spray Trials**

Initial spray trials of single, thin coating applications were conducted whereby different wires were sprayed onto BAAM substrates for a coarse evaluation of feasibility. It was expected that a direct application of a harder, higher melting temperature material would not be able to be directly applied to the BAAM without an intermediate layer so several softer, lower melting temperature materials with tested as well, namely Zinc, Aluminum, and Copper. Images of results from some of these initial spray trials are shown in *Figure 5*.

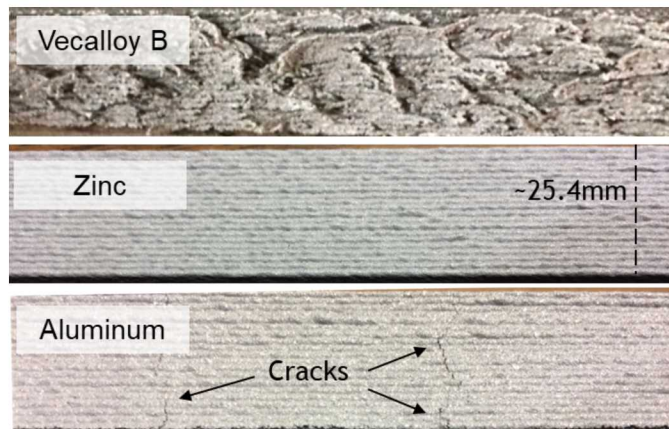


**Figure 5: Top surface images of ~25.4mm x ~229mm ABS/CF-20% BAAM substrates coated with Vecalloy B, Zinc, and Aluminum with varying degrees of adhesion and coating integrity.**

The Vecalloy B wire coating was very poorly adhered, with several cracks and flaked off material. It was assumed that other wires of harder material (“Amorphous Alloy”, “WC Amorphous” and High Carbon Steel) would behave similarly and were not tested. Of the lower melting temperature materials, Zinc showed the best coatings quality and visually observed adherence. Aluminum adhered well but macroscopic cracks were observed on the coating surface, which were expected to harm coating adhesion with greater thickness. Secondary layers of other wires were able to be deposited on top of the Zinc coating with greater success than without the Zinc layer, demonstrating the usefulness of Zinc as a bond coat.

BAAM surfaces were sprayed in both the as-received condition and with grit blasting. Whereas grit blasting is typically performed on metallic substrates to roughen the surface to promote mechanical adherence, grit blasting seemed to smooth the BAAM surface as the blast media eroded the material. The natural texture of the BAAM material included a macroscopic roughness that may aid in the mechanical anchoring of the Zinc coatings. The cross-section micrograph shown in *Figure 6* illustrates the ability of the Zinc coating to infiltrate the native roughness of the printed BAAM material.

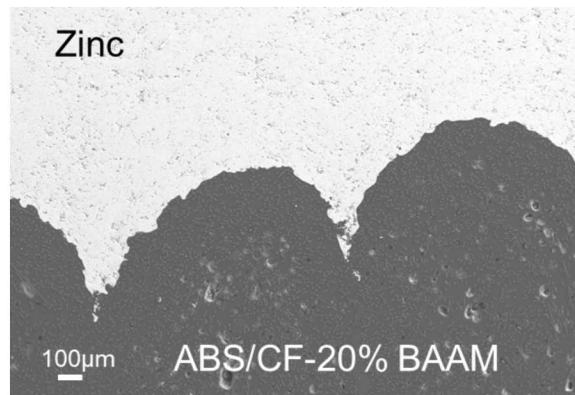


**Figure 6: Cross section micrograph of the interface between TWA Zinc coating and the ABS/CF-20% BAAM substrate. The Zinc coating readily infiltrates the roughness of the BAAM material that is native to the printing process, promoting mechanical adhesion.**

At the end of the initial spray trials for material screening, it was decided to pursue a dual layered approach to reach the goal of producing a hard and durable metallized BAAM surface. TWA Zinc would be applied directly to the BAAM substrate without any additional surface preparation. The Zinc layer would then be followed by a harder top coat material. It was decided to pursue the “WC Amorphous” and “Amorphous Alloy” for microstructural examination. These two materials were selected based on their product sheets citing hardness near tool steel (65 Rockwell Hardness C (HRC) for “WC Amorphous” and 50-55 HRC for amorphous Alloy”) which eliminated the High Carbon Steel (cited at 20-25 HRC on its product sheet). Also informing this down select was the high residual stress observed for the Vecalloy B wire (which was showing delamination would delaminate from Aluminum test substrates).

### **2.1.3. Coating Microstructure and Hardness Characterization**

Cross sections of thick Zinc, “WC Amorphous”, and “Amorphous Alloy” were prepared and characterized by Scanning Electron Microscope (SEM). *Figure 7* shows the cross section of the Zinc bond coat material. A large amount of porosity is observable within the microstructure but does not include easily discernable secondary phases of oxides

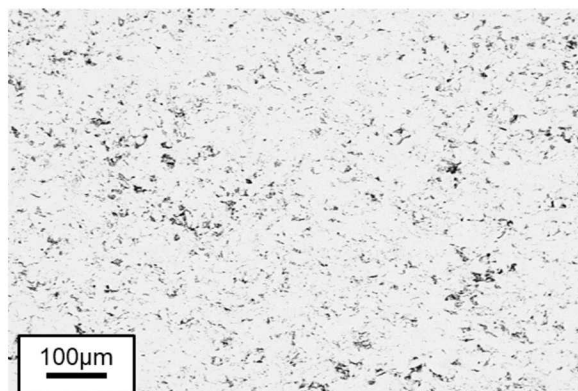


**Figure 7: Cross section SEM micrograph of thick TWA Zinc coating.**

SEM micrographs of the “WC Amorphous” and “Amorphous Alloy” sprayed onto Aluminum substrates are shown in *Figure 8*. Both coatings showed a typical sprayed microstructure consisting of lamellar “splats” from the molten droplet deposition. Microcracks and pores are readily observable as well in the darker regions of the micrographs. Detail features of the coating microstructure were evaluated by Electron Dispersive Spectroscopy (EDS). The “WC Amorphous” coatings consisted of large WC particles (The whitest regions of the micrographs) and smaller particles of TiC embedded within a primarily Fe-Cr-Ni matrix. The “Amorphous Alloy” consisted primarily of a Fe-Cr-Ni-Mo-Cu matrix, with some regions of Cr concentration in the darker grey regions of the micrograph.

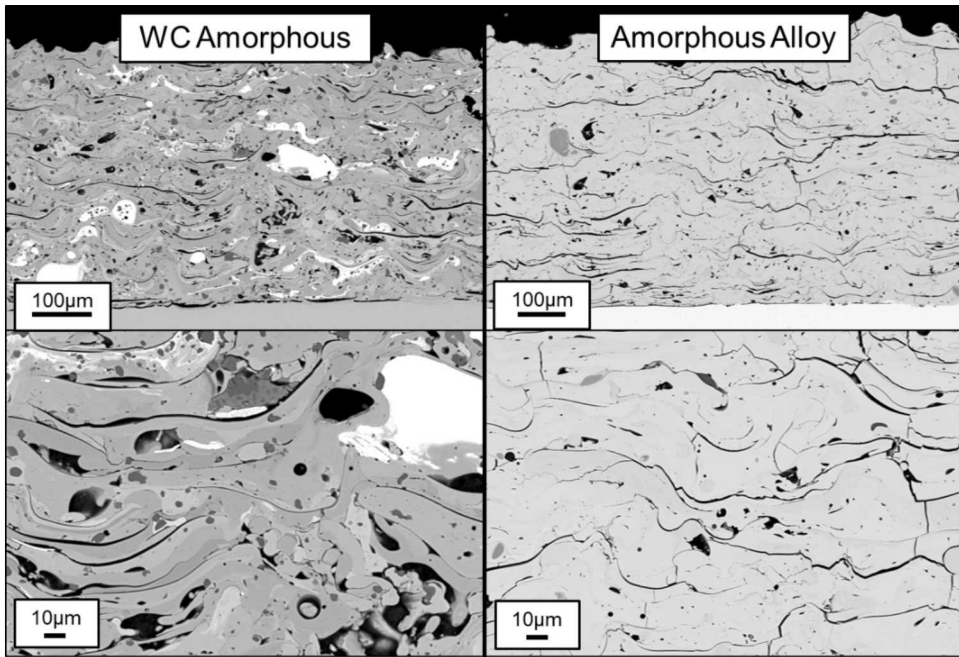


**Figure 8: Cross section SEM micrographs of the “WC Amorphous” and “Amorphous Alloy” coatings.**

Vickers hardness testing was performed on the top surface of the coatings to assess how the sprayed material compares to materials used for tooling. The coatings were mounted in metallographic epoxy and polished to a mirror finish prior to testing. A 0.3kgf load was used to indent the samples and hardness was calculated by measuring the average length of the diagonals of the indent. The results of 165 hardness tests are shown in *Figure 9*. Both coatings have significant scatter in the results which is likely a result of the non-homogenous and defect containing microstructure innate in TWA coatings. Further optimization and densification of the spray process may tighten the distribution of hardness measurements. Both coatings show an average Vickers hardness (HV) of ~600 HV, which is roughly equivalent to ~55 HRC (O1 Tool Steel is typically used in the range of 61-63 HRC).

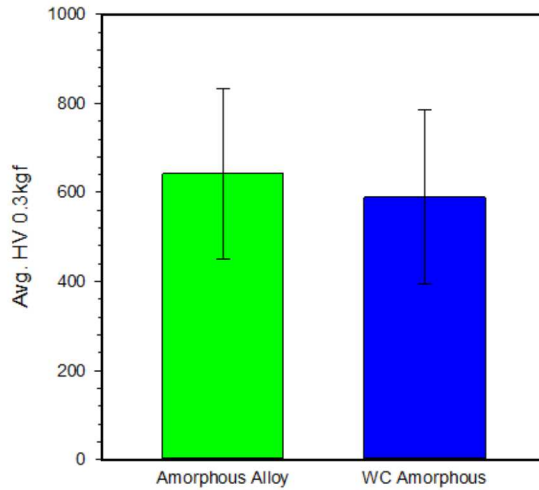


**Figure 9: Average Vickers hardness measured for the “Amorphous Alloy” and “WC Amorphous” coating top surfaces with error bars showing the standard deviation.**

In-plane Vickers hardness was also measured for the top coat materials using prepared cross sections. The results of 20 measured indents are shown in *Figure 10*. Again, significant spread in the data is observed owing to the non-homogeneity of the coating microstructures. A slightly higher average hardness is observed in cross section compared to top surface but is well within the standard deviation of the data.

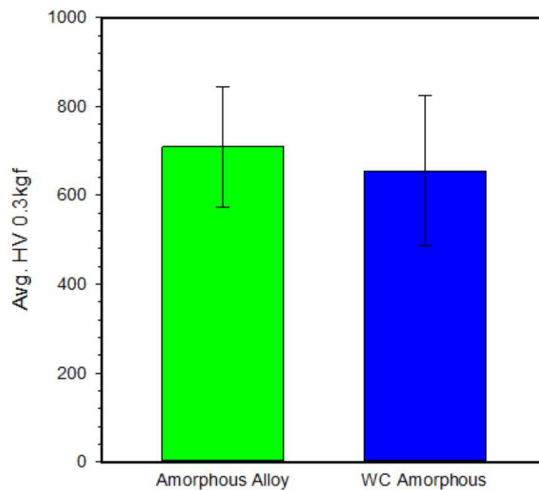


**Figure 10: Average Vickers hardness measured for the “Amorphous Alloy” and “WC Amorphous” coating cross sections with error bars showing the standard deviation.**

## 2.2. Task 2: Optimize Electric Arc Spray Process for Low Coating Residual Stress and High Adhesion Strength

Varying process parameters in the TWA spray process changes the characteristics of the particles it creates, such as droplet size, temperature, and velocity, which are known to have an influence on the

microstructural characteristics of the coating and are commonly studied with thermal spray processes<sup>3,4</sup>. Using such resources, a spray parameter was used that would maximize coating density while minimizing coating roughness. However, the limitations of the TWA process preclude having a fully dense coating and typically produce coatings with an average roughness (Ra) on the order of 10-20 $\mu\text{m}$  Ra. It is expected that a higher velocity spray process would produce denser coating but that some sort of grinding or finishing would still be necessary for tooling applications.

### 2.2.1. **Residual Stress Characterization**

The TWA coating process has an inherent tensile coating stress during deposition owing to molten droplet quenching and shrinkage. Thermal expansion mismatch between the coating and substrate also contributes an element to the residual stress of the coating when the coating-substrate system cools back to room temperature after coating deposition. This thermal stress may help neutralize the tensile stress that occurs from deposition if the Coefficient of Thermal Expansion (CTE) of the substrate is greater than the coating material and the coating-substrate system can heat up during deposition. Since the BAAM substrates do not have as much thermal tolerance as metallic substrates that are typical in TWA coating applications, using the thermal strain to neutralize the coating stress did not seem feasible.

Measurements using the ICP sensor were attempted during TWA coating of the BAAM substrates to quantify coating in-plane residual stress. However, the irregularity in the thickness of the 25.4mm x 229mm beams and not knowing the thermo-mechanical properties of the BAAM materials (Modulus, Poisson Ratio, CTE) made it difficult to compute coating residual stresses in the typical manner using the substrate curvature and Stoney formula, shown below in Equation 1, where  $\sigma_{Film}$  is the in-plane coating residual stress,  $E'_s$  (equal to  $E_s/(1-\nu)$  where  $\nu$  is Poisson ration and  $E_s$  is substrate Modulus) is the substrate bi-axial stiffness,  $\Delta K$  is change in substrate curvature,  $H$  is substrate thickness, and  $h$  is coating thickness.

$$\sigma_{Film} = \frac{E'_s H^2 \Delta K}{6h} \quad (1)$$

Tests with the ICP sensor were performed using Aluminum substrates with uniform thicknesses instead of the BAAM substrates in order quantify the residual stresses of the TWA wire coatings. It can be expected that there would be differences in residual stress between coatings deposited on Aluminum and BAAM Polymers due primarily to their differences in CTE and secondarily to their thermal conductivity; A polymer substrate will not remove the heat from molten droplets away as quickly as a metallic substrate, making a larger thermal gradient throughout the substrate-coating system and possibly altering the droplet's solidification behavior for the first layer of droplets. Curvature and temperature data measured by the ICP sensor for TWA sprayed Zinc onto an Aluminum substrate is shown in Figure 11. Five coating passes were applied to the substrate in a robotically controlled X-Y raster pattern, corresponding to the curvature and temperature peaks. Smaller undulations within those peaks correspond to the successive steps within the X-Y pattern to ensure uniform coating application over the area of the substrate. These five coating passes amounted to a Zinc coating with a thickness of  $\sim 860\mu\text{m}$ . Using Equation 1, the residual stress of the coating was approximated to be  $\sim 5$  MPa.

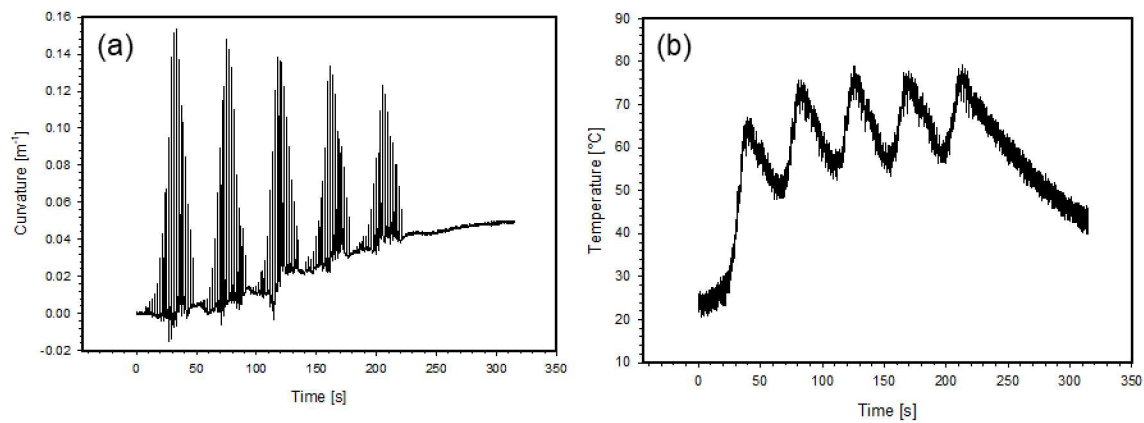


**Figure 11: ICP measurements for TWA sprayed Zinc onto Aluminum (a) Curvature vs. time and (b) backside substrate temperature vs. time. Measurements were taken simultaneously during coating deposition and cooling.**

Top coats of “WC Amorphous” and “Amorphous Alloy” were applied as a single pass to the Zinc coated Aluminum substrates and measured using the ICP sensor to get a sense of the anticipated stresses from the top coats and are shown in *Figure 12* and *Figure 13*, respectively. It is easily seen that a much greater amount of substrate curvature is induced by the single top coat passes than for the Zinc coatings while also depositing a lower amount of coating material ( $\sim 100\mu\text{m}$  were deposited for both top coats). Residual stresses were approximated to be on the order of 100 MPa for these top coat materials.

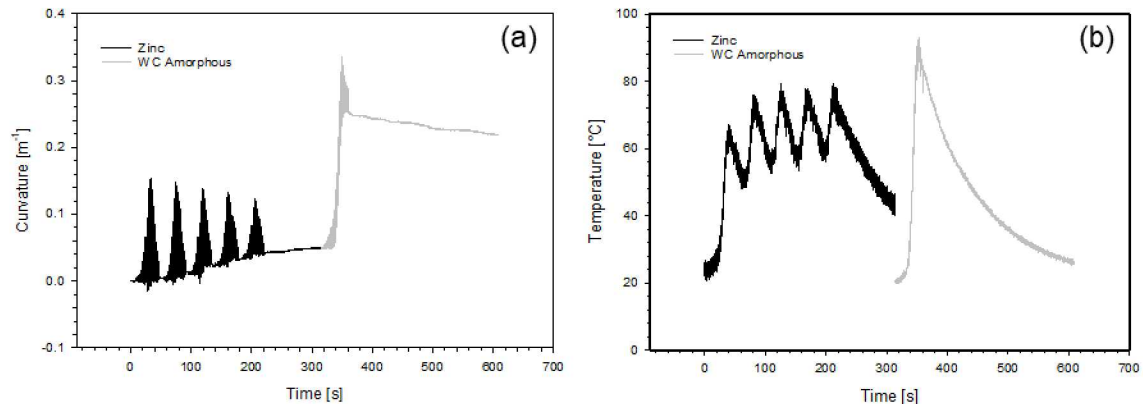


**Figure 12: ICP measurements for TWA sprayed “WC Amorphous” wire onto TWA Zinc coated Aluminum (a) Curvature vs. time and (b) backside substrate temperature vs. time. Measurements were taken simultaneously during coating deposition and cooling.**

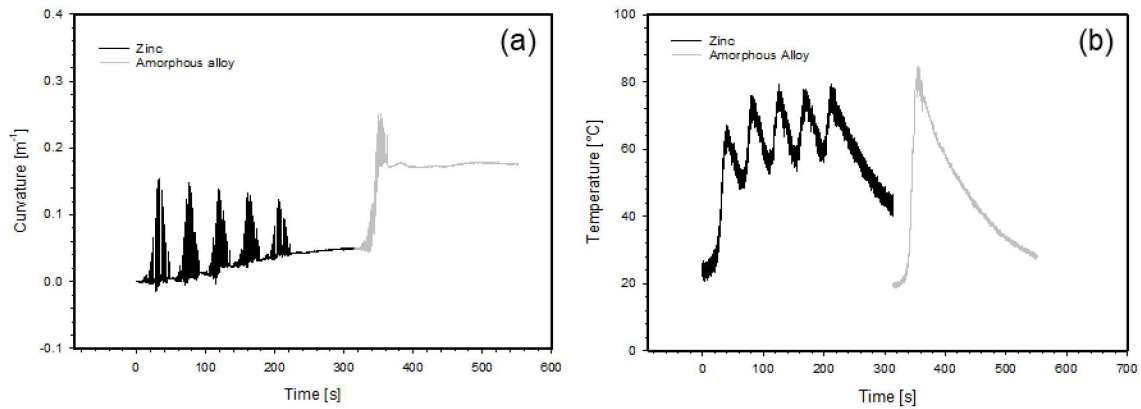


**Figure 13: ICP measurements for TWA sprayed “WC Amorphous” wire onto TWA Zinc coated Aluminum (a) Curvature vs. time and (b) backside substrate temperature vs. time. Measurements were taken simultaneously during coating deposition and cooling.**

The large contrast in residual stresses between the Zinc bond coat and top coat materials are evident and may indicate why Zinc readily adheres to the BAAM Polymer substrates. The specific mechanism for TWA Zinc having such a low residual stress is unknown, but may be related to the material’s high homologous temperature during coating deposition and the known ability of pure Zinc to recover yield points from deformation near room temperature<sup>5</sup>.

### 2.2.2. Optimization for Coating Adhesion

It was conceived that a thicker layer of the soft, low residual stress Zinc bond coat could act as a stress buffer by accommodating the higher stresses of the top coats, reducing the shear force applied to the interface of the BAAM polymer. A simple experiment was conducted where the Vecalloy B wire (which was abandoned for further studies due to its high residual stress) would be applied to the native BAAM surface, a BAAM substrate that had a single Zinc layer applied, and a BAAM substrate with several Zinc layers applied. An image of the resulting top surfaces is shown in *Figure 14*. The sample without any Zinc bond coat is the same as that shown in *Figure 5*, where severe flaking and delamination of the coating occurred during deposition. With the thin layer of Zinc, the coating fractured in the middle and peeled from the edges. The Vecalloy B maintained adhesion with the Zinc, exposing the BAAM polymer surface in the areas where the coating had peeled. With the thicker layer of Zinc bond coat the Vecalloy B - Zinc coating system remained largely adhered to the substrate with only minor delamination at corners observed.

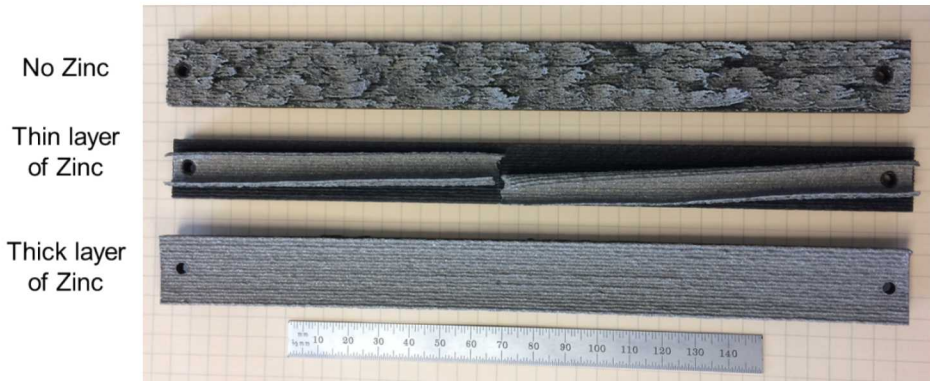


**Figure 14: Top surfaces of BAAM Polymer coupons that we sprayed with Vecalloy B with no Zinc bond coat, a thin Zinc bond coat, and a thick Zinc bond coat.**

Measurement of adhesion for thermal spray coatings is typically carried out using an ASTM C633 test, where the top surface of a circular plug is coated and glued to another plug and pulled apart by a tensile test to determine bond strength. However, with the irregularity of the substrate surface from the printed beads of the BAAM polymer it was not believed that this test would provide useful information.

### 2.2.3. Coating Roughness

In addressing the coating roughness reduction that would be necessary to reach a machine finish for tooling application, there are two aspects that need to be addressed: The macroscopic topography of the printed BAAM polymer surface and the microscopic roughness from the droplet solidification. The macroscopic roughness of the beaded substrate surface is thought to enhance mechanical adhesion of the Zinc bond coat, so it was decided to not machine the substrate surface prior to coating application. Instead, machining of the Zinc layer by an end mill was performed and successfully levelled the coating surface without un-due damage to the Zinc layer. A top coat was applied to a sample that had a portion zinc layer levelled and the other portion left as the native surface to ensure that the top coat would still adhere. An image of this sample is shown in *Figure 15*.

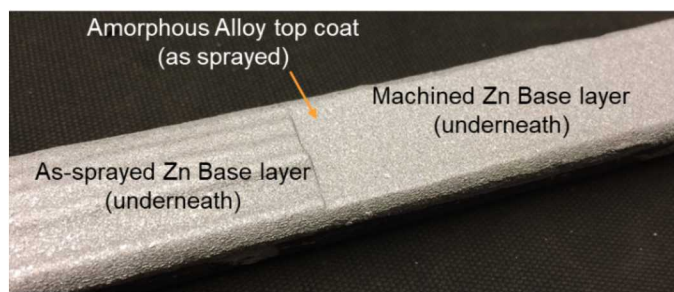


**Figure 15: Sample where the Zinc bond coat was machined on half of the surface prior to top coat application.**

The micro roughness of the harder top coat can be reduced through grinding and polishing or diamond machining, which would be necessary for a machine quality finish. An image of a small ground and polished sample is shown in *Figure 16* and a larger diamond machined sample with the steps of a proposed stack up is shown in *Figure 17*.

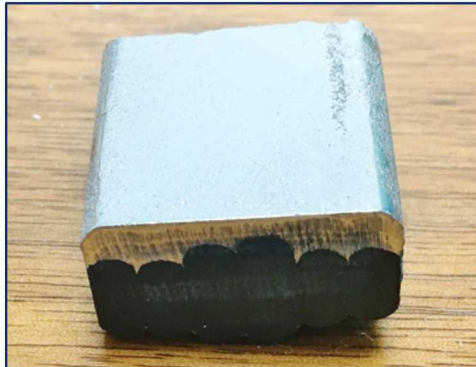


**Figure 16: Sample of metallized BAAM Polymer with a Zinc bond coat that has been machined flat, followed by a polishing “Amorphous Alloy” top coat.**

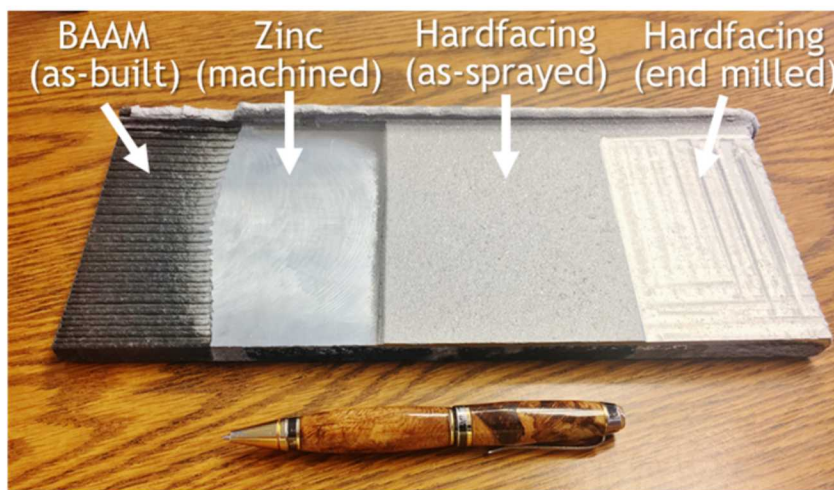


**Figure 17: Sample plate that highlights the steps of a proposed stack up for BAAM metallization.**

### **2.3. Task 3: Fabrication and Compression Testing of Simple Geometry Tooling**

Fabrication and compression testing of the TWA metal coatings on BAAM polymer substrates was desired to assess both the feasibility of the process to coat relevant tooling geometries as well as the performance of such a material system under relevant loads. Compression tests were done by Brinell indentation of the material stack-ups previously described. A simple tooling design was printed by ORNL for SNL to coat to demonstrate processing feasibility for simple tool designs.

#### **2.3.1. Compression Test by Brinell Indentation**

Vickers hardness (with a 300g load) is commonly employed for measuring the quality of thermal spray coatings, particularly in hard facing and wear resistant applications. These tests are typically measured on the cross section of the coatings and reflect a combination of both the intrinsic coating material hardness and the degree of consolidation of the sprayed material. The hardness of the

surface under a compressive test is of greater value for a tooling application, particularly when consisting of a multi-layered structure as in the metallized BAAM polymer. Literature has reported several studies whereby an adaptation of Brinell hardness is used and analyzed by the Tabor Method to produce compressive stress-strain curves for spray coatings<sup>6,7,8</sup>. Material selection, processing methods, and operating parameters (in order of significance) all show influences on coatings' compressive behavior. It was concluded that a Brinell test could be a simple but good measurement of the effectiveness of the coating method's compressive strength and adhesion.

Samples we made on both the ABS/CF-20% and PPS/CF-50% BAAM polymer substrates. A significantly thick Zinc layer was deposited directly to the polymer surface to allow planarizing the surface by end milling and still allow a thick enough coating to allow adhesion of the "Amorphous Alloy" and "WC Amorphous" top coated materials that were sprayed to ~0.5mm thickness. The top coats were left with their native as-sprayed surface roughness for the Brinell indentation tests. Zinc coatings and un-coated BAAM polymers substrates were also tested as a comparison. A 10mm diameter steel ball was loaded onto the material surfaces at a load of 500kg. Indent diameters were measured by a Keyence profilometer to the closest 0.1mm, allowing the Tabor method to calculate the mean pressure and representative strain using Equation 2 and Equation 3, respectively, where L is the indenter load, a is the radius of the plastically deformed area, and R is the indenter tip radius

$$\text{Mean Pressure} = \frac{L}{\pi a^2} \quad (2)$$

$$\text{Representative Strain} = 0.2 \frac{a}{R} \quad (3)$$

Single points of Mean Pressure vs. Representative Strain of the coated and un-coated PPS/CF-50% BAAM Polymer is shown in Figure 18. The Zinc coating alone performed worse than the un-coated substrate by having a larger indent area from the same load and the ability to withstand a lower mean pressure. Testing of the "Amorphous Alloy" and "WC Amorphous" top coats (including the Zinc bond coat beneath) performed better than the un-coated substrate with a higher mean pressure allowing less plastic strain. A more robust compression stress-strain curve could be produced by measuring multiple indents over a range of indenter loads. However, this simple test confirmed an improvement to surface hardness by using the Zinc + top coat approach made by TWA spraying. This is also an over test of anticipated pressures anticipated for stretch forming and compression forming tools would be <3000psi (~20MPa).

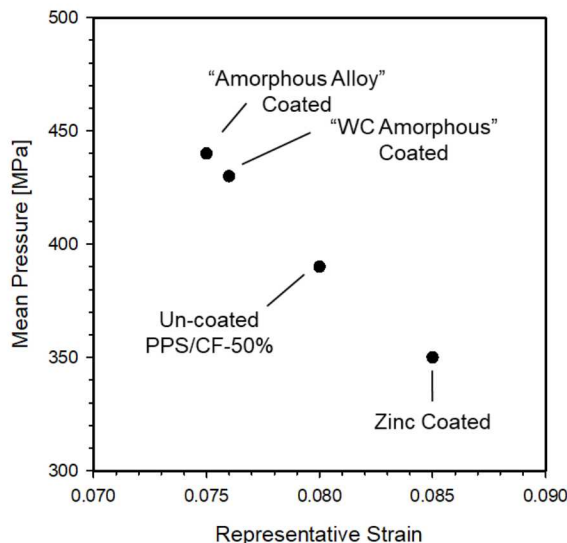


**Figure 18: Representative Strain vs. Mean Pressure for coated and un-coated PPS/50% CF BAAM Polymer.**

The ABS/CF-20% substrates experienced catastrophic cracking in areas between the beads from printing in both the un-coated and coated state, preventing proper analysis. Coating remained largely adhered even though significant substrate cracking had occurred.

Metallographic cross sections of the indented areas were prepared for the "Amorphous Alloy" and "WC Amorphous" containing samples and are shown in *Figure 19* and *Figure 20*, respectively. From the micrographs, it is clear to see that both top coats have undergone significant deformation and cracking from the indentation, though the nature of the cracking varies between the two top coat materials with the "Amorphous Alloy" has a greater density of cracks than the "WC Amorphous". No significant de-bonding between any of the layers was evident in these micrographs.

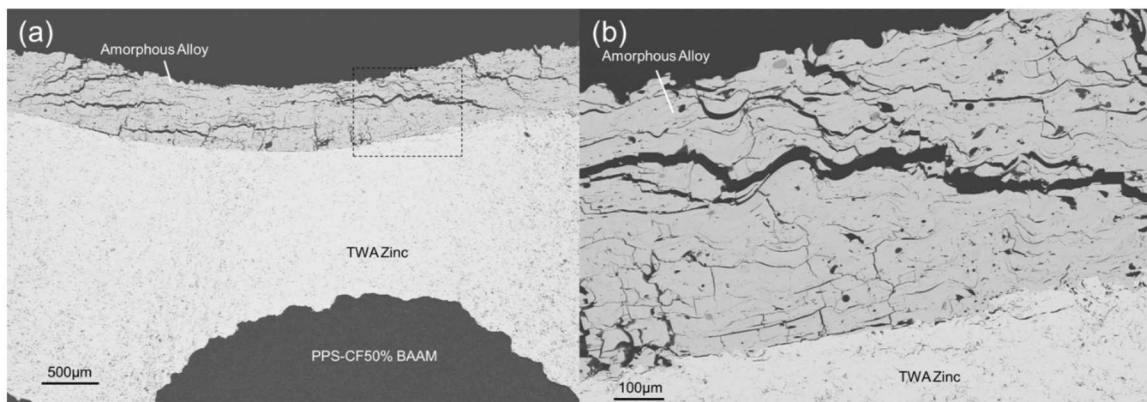


**Figure 19: Micrographs of the indented area of the "Amorphous Alloy" on TWA Zinc on PPS-CF 50% BAAM. (a) Larger scale image of coating layers and damage with highlighted area (b) showing greater detail of top coat damage**

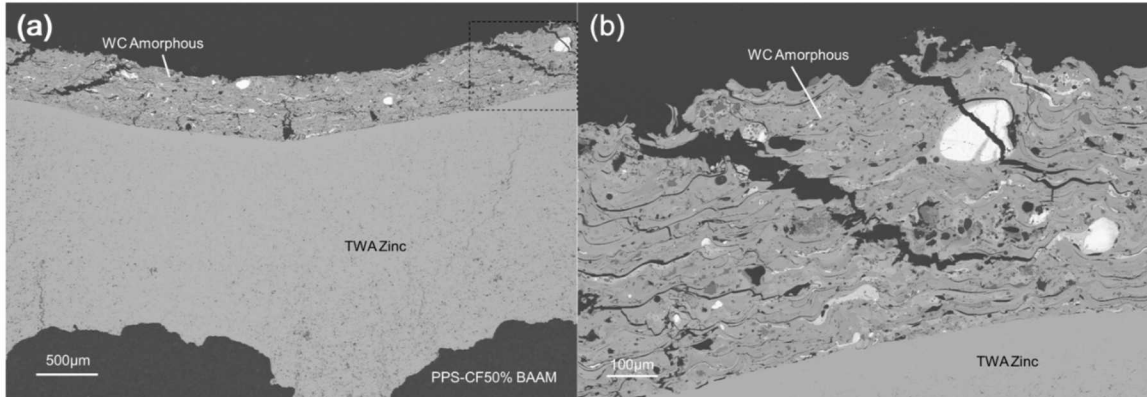


**Figure 20: Micrographs of the indented area of the “WC Amorphous” on TWA Zinc on PPS-CF 50% BAAM. (a) Larger scale image of coating layers and damage with highlighted area (b) showing greater detail of top coat damage.**

In addition to top coat damage, micrographs of the TWA Zinc layer (shown in *Figure 21*) reveal changes in the microstructure as well. Both samples show apparent densification of the Zinc underneath the indentation, but also appears to be dependent on the location of the BAAM height vs. indenter. The TWA Zinc layer underneath the “WC Amorphous” topcoat also showed a series of vertical cracks along the boundary of the densified Zinc with the unaffected Zinc areas, indicated by arrows in *Figure 21 (b)*

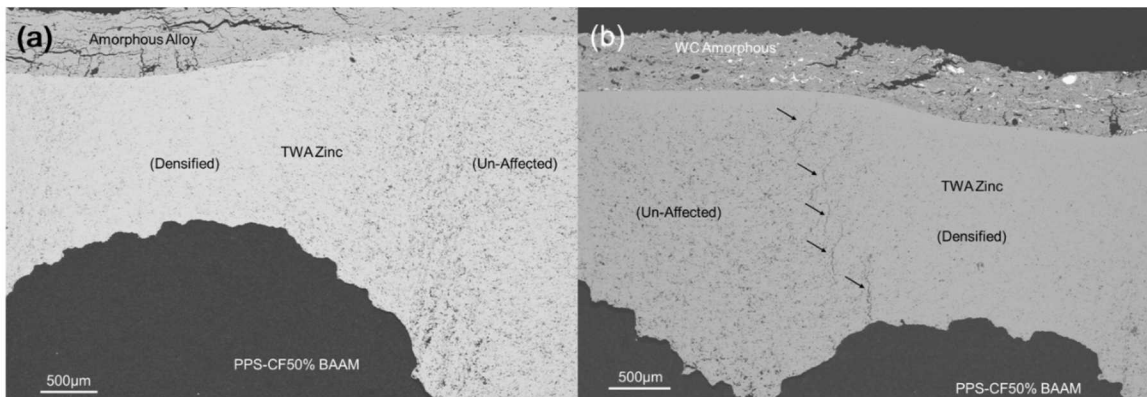


**Figure 21: Micrographs featuring damage done to the TWA Zinc bond coat underneath the (a) “Amorphous Alloy” and (b) “WC Amorphous” top coats. Arrows indicate cracks in the Zinc in (b)**

Further optimization in compressive strength could be potentially achieved using different top coat materials, different processing methods for denser deposits, and an optimization of layer thickness based on the compromise between adhesion strength and hardness.

### 2.3.2. **Fabrication of Coating on Simple Geometry Tooling**

Simple geometry tooling consisting of a convex and a concave faced BAAM PPS/CF-50% block was printed by ORNL’s MDF and sent to SNL’s TSRL for coating. Images of the uncoated parts are shown in *Figure 22*. The blocks were approximately 200mm sided cubes



**Figure 22: Convex (Left) and Concave (Right) simple geometry tooling blocks BAAM printed in PPS/CF-50%.**

Coating of the blocks was done with a thick Zinc bond layer and the “Amorphous Alloy” top coat. A photo of a block after the Zinc application is shown in Figure 23. The block face was slightly angled to be off-normal to the spray application to let the coating wrap around the side walls of the block to reduce potential edge effects during a test stamping. The block angle was switched back and forth to ensure equal coating on the side walls. An attempt to smooth the Zinc coating by hand was made to eliminate the persistence of macro-roughness from the print beads. A more complex grinding operation would be required for complete smoothing in an application but was not possible due to machining limitations at TSRL.



**Figure 23: Simple geometry tooling block after Zinc coating.**

### **3. ACCOMPLISHMENTS AND CONCLUSIONS**

This project successfully demonstrated a pathway for hard-facing metallization of BAAM polymers using the cheap and high throughput TWA process.

#### **3.1. Patents**

Sandia National Labs Technical Advance SD#14687 – “Hardfacing of Additively Manufactured Polymer via Twin Wire Arc Spray”

#### **3.2. Publications and Presentations**

A.Vackel, M.Smith, A.Miller, C. Profazi, “Multi-layer Metallization of Polymer Materials via Thermal Spray” International Conference on Metallurgical Coatings and Thin Films 2018, San Diego, CA. April 24<sup>th</sup>, 2018.

A.Vackel, M.Smith, A.Miller, C. Profazi, “Multi-layer Metallization of Polymer Materials via Thermal Spray” International Thermal Spray Conference 2018, Orlando, FL. May 8<sup>th</sup>, 2018.

A.Vackel, J.Fonseca, A.Miller, “Thermal Spray Deposition of Refractory Metals and Alloys on Polymer Materials” 44<sup>th</sup> Polymeric Materials, Adhesives, and Composites Meeting, Sandia National Labs, Albuquerque NM. June 26<sup>th</sup>, 2018.

#### **3.3. Recommendations**

Several future efforts could be undertaken to optimize the process for specific applications as described below

- Top coat materials: Due to limit in scope, this effort utilized commercial off the shelf feedstock wires that are used for typical hard facing applications where TWA is a firmly established technology. The primary focus of such hard facing wires are for abrasive resistance and not for a tooling application. Future work could focus on sourcing or formulating specific feedstock wire for tooling applications.
- Coating density: While TWA provides a high application rate at a lower cost than most thermal spray technologies, the primary trade-off is coating porosity due to slower particle velocities. This porosity lowers the hardness and durability of a coating. Recently developed technologies offer a hybrid High Velocity-TWA process that produces denser coatings and may be considered for making harder top coats.
- Layer thickness optimization: Determining the optimum bond coat and top coat layer thicknesses in a balance of adhesion and hardness should be determined depending on applications.

#### 4. REFERENCES

1. Kuroda, Seiji, et al. "Peening action and residual stresses in high-velocity oxygen fuel thermal spraying of 316L stainless steel." *Journal of thermal spray technology* 10.2 (2001): 367-374.
2. Matejicek, J., and S. Sampath. "In situ measurement of residual stresses and elastic moduli in thermal sprayed coatings: Part 1: apparatus and analysis." *Acta Materialia* 51.3 (2003): 863-872.
3. Johnston, Allison Lynne, Aaron Christopher Hall, and James Francis McCloskey. "Effect of process inputs on coating properties in the twin-wire arc zinc process." *Journal of thermal spray technology* 22.6 (2013): 856-863.
4. Horner, Allison, Aaron Hall, and James McCloskey. "The effect of process parameters on twin wire arc spray pattern shape." *Coatings* 5.2 (2015): 115-123.
5. Wain, Henry Laurence, and A. H. Cottrell. "Yield Points in Zinc Crystals." *Proceedings of the Physical Society. Section B* 63.5 (1950): 339.
6. Prchlik, Lubos, Jan Pisacka, and Sanjay Sampath. "Deformation and strain distribution in plasma sprayed nickel-aluminum coating loaded by a spherical indenter." *Materials Science and Engineering: A* 360.1-2 (2003): 264-274.
7. Choi, W. B., et al. "Integrated characterization of cold sprayed aluminum coatings." *Acta Materialia* 55.3 (2007): 857-866.
8. Choi, W. B., et al. "Indentation of metallic and cermet thermal spray coatings." *Journal of thermal spray technology* 18.1 (2009): 58-64.



## DISTRIBUTION

### Hardcopy—Internal

Number of Copies	Name	Org.	Mailstop
1	Andrew S. Miller	01834	1130
1	Andrew Vackel	01834	1130

### Email—External [REDACTED]

Name	Company Email Address	Company Name
Ahmed Hassen	<a href="mailto:hassenaa@ornl.gov">hassenaa@ornl.gov</a>	Oak Ridge National Lab
Vlastimil Kunc	<a href="mailto:kuncv@ornl.gov">kuncv@ornl.gov</a>	Oak Ridge National Lab
John Lindahl	<a href="mailto:lindahljm@ornl.gov">lindahljm@ornl.gov</a>	Oak Ridge National Lab
David Nuttall	<a href="mailto:nuttalld@ornl.gov">nuttalld@ornl.gov</a>	Oak Ridge National Lab
William Peter	<a href="mailto:peterwh@ornl.gov">peterwh@ornl.gov</a>	Oak Ridge National Lab
Brian Post	<a href="mailto:postbk@ornl.gov">postbk@ornl.gov</a>	Oak Ridge National Lab

### Email—Internal

Name	Org.	Sandia Email Address
Joe Fonseca	01834	<a href="mailto:jcfonse@sandia.gov">jcfonse@sandia.gov</a>
Michael Leap	01834	<a href="mailto:mjleap@sandia.gov">mjleap@sandia.gov</a>
Neiser, Richard	01830	<a href="mailto:raneise@sandia.gov">raneise@sandia.gov</a>
Andrew S. Miller	01834	<a href="mailto:amille1@sandia.gov">amille1@sandia.gov</a>
Christina Profazi	01819	<a href="mailto:caprofa@sandia.gov">caprofa@sandia.gov</a>
Randall Schunk	01815	<a href="mailto:prschun@sandia.gov">prschun@sandia.gov</a>
Andrew Vackel	01834	<a href="mailto:avackel@sandia.gov">avackel@sandia.gov</a>
Technical Library	01177	<a href="mailto:libref@sandia.gov">libref@sandia.gov</a>

This page left blank

This page left blank



**Sandia  
National  
Laboratories**

Sandia National Laboratories is a multimission laboratory managed and operated by National Technology & Engineering Solutions of Sandia LLC, a wholly owned subsidiary of Honeywell International Inc. for the U.S. Department of Energy's National Nuclear Security Administration under contract DE-NA0003525.